Mon. Not. R. Astron. Soc. **362,** 1273–1278 (2005) doi:10.1111/j.1365-2966.2005.09394.x

High-resolution extreme ultraviolet spectroscopy of G191-B2B: structure of the stellar photosphere and the surrounding interstellar medium

M. A. Barstow,[1⋆] R. G. Cruddace,[2] M. P. Kowalski,[2] N. P. Bannister,[1] D. Yentis,[2] J. S. Lapington,[1] J. A. Tandy,[3] I. Hubeny,[4,5] S. Schuh,[6] S. Dreizler[6] and T. W. Barbee[7]

[1]*Department of Physics and Astronomy, University of Leicester, University Road, Leicester LE1 7RH*
[2]*E.O. Hulburt Center of Space Research, Naval Research Laboratory, Washington DC 20375, USA*
[3]*Mullard Space Science Laboratory, University College London, Holmbury St Mary, Dorking, Surrey RH5 6NT*
[4]*National Optical Astronomy Observatories (NOAO), Tucson, AZ 85726, USA*
[5]*Steward Observatory, University of Arizona, Tucson, AZ 85721, USA*
[6]*Institut für Astrophysik, Universität Göttingen, Friedirch-Hund-Platz 1, D-37077 Göttingen, Germany*
[7]*Lawrence Livermore National Laboratory, Livermore, CA 97550, USA*

Accepted 2005 July 1. Received 2005 June 29; in original form 2004 July 30

ABSTRACT

We have continued our detailed analysis of the high-resolution ($R = 4000$) spectroscopic observation of the DA white dwarf G191-B2B, obtained by the *Joint Astrophysical Plasmadynamic Experiment* (*J-PEX*) normal incidence sounding rocket-borne telescope, comparing the observed data with theoretical predictions for both homogeneous and stratified atmosphere structures. We find that the former models give the best agreement over the narrow waveband covered by *J-PEX*, in conflict with what is expected from previous studies of the lower resolution but broader wavelength coverage *Extreme Ultraviolet Explorer* spectra. We discuss the possible limitations of the atomic data and our understanding of the stellar atmospheres that might give rise to this inconsistency. In our earlier study, we obtained an unusually high ionization fraction for the ionized He II present along the line of sight to the star. In the present paper, we obtain a better fit when we assume, as suggested by Space Telescope Imaging Spectrograph results, that this He II resides in two separate components. When one of these is assigned to the local interstellar cloud, the implied He ionization fraction is consistent with measurements along other lines of sight. However, the resolving power and signal-to-noise available from the instrument configuration used in this first successful *J-PEX* flight are not sufficient to clearly identify and prove the existence of the two components.

Key words: stars: atmospheres – white dwarfs – ISM: general – ultraviolet: stars.

1 INTRODUCTION

As one of the brightest and best-studied hot white dwarfs, G191-B2B has been an important benchmark to test the physics incorporated into atmosphere models, which can then be applied to the study of other objects. Observations of this star and what it tells us about white dwarf evolution have been reported in many papers (e.g. Sion et al. 1992; Vennes et al. 1992; Holberg et al. 1994; Barstow, Hubeny & Holberg 1998, 1999; Dreizler & Wolff 1999).

In an earlier paper (Cruddace et al. 2002), we presented an analysis of the extreme ultraviolet (EUV) spectrum of G191-B2B, obtained in a sounding rocket flight of the *Joint Astrophysical Plasmadynamic Experiment* (*J-PEX*) high-resolution spectrometer. Using a model stellar atmosphere which assumed a homogeneous composition and incorporating interstellar absorption, the principal result was the clear detection of a low-density ionized He component along the line of sight, which had only previously been inferred from lower-resolution observations with the *Extreme Ultraviolet Explorer* (*EUVE*). However, the estimated ionization fraction of He (∼0.7) was unusually high. Inclusion of a significant abundance of photospheric He yielded a best fit to the spectrum, and excluded at the 99 per cent confidence level solutions in which He was absent. However, the implied He/H abundance of 1.6×10^{-5} (by number) did not yield photospheric lines that were strong enough to be detected directly at the signal-to-noise of the *J-PEX* spectrum.

⋆E-mail: mab@star.le.ac.uk

We present a new analysis of this *J-PEX* spectrum, which considers a wider range of possible models developed in earlier studies. These include homogeneous atmosphere models, in which heavy element compositions have been updated in the light of recent UV studies (Barstow et al. 2003), and stratified structures determined from both empirical matches to the *EUVE* spectrum (Barstow et al. 1999) and a self-consistent treatment of the radiative levitation forces (Schuh, Dreizler & Wolff 2002). This work includes an improved treatment of the wavelength calibration, which takes into account second-order errors in the solution that were not dealt with originally. Further, we re-examine the interstellar absorption in the light of Space Telescope Imaging Spectrograph (STIS) results (discussed in Section 4.2), which indicated that the low-density ionized He material may in fact reside in two components at different locations along the line of sight.

2 DATA REDUCTION

The *J-PEX* spectrometer has been described briefly by Cruddace et al. (2002) and will be discussed in more detail in a forthcoming paper (Cruddace et al., in preparation). The stellar spectrum appears as four offset lines across the detector image, each covering a similar wavelength range. The image is then corrected for pointing drifts before the spectra are extracted from it. Using laboratory calibration images of a Penning discharge source, an approximate wavelength scale was established for each spectrum, which was fitted by a third-order polynomial. The final wavelength scale for each spectrum was established by cross-correlation with the G191-B2B *EUVE* medium wavelength spectrum. This process also allowed us to determine the wavelength scale offsets for the gratings, which were then refined by cross-correlating the individual spectra with each other to find common spectral features. Finally, the raw spectra were corrected for all offsets and rebinned to a common 0.04-Å grid for analysis. Inspection of the original reduction, reported by Cruddace et al. (2002), reveals that the predicted locations of some reliably identifiable features disagree slightly with their observed positions, and we have taken these features into account to make small adjustments to the wavelength scale.

Pre-flight dark exposures revealed a detector noise count rate of less than five counts s^{-1} over the entire imaging area. Hence, the mean count per spectral bin accumulated during the 300-s exposure is sufficiently low that the stellar spectra could be assumed to be free of background. As a result of unexpected shifts, during launch, in the relative alignment of the spectrometer and the attitude control system star tracker, only two spectra were registered with the full wavelength range within the detector active area, while two were cut off by the detector boundary at ∼239 Å. Hence, between 239 and 243 Å only half the geometric collecting area of the telescope was used, effectively halving the exposure by comparison with the shorter wavelengths. To maintain a roughly constant signal-to-noise across the whole spectrum, data in this range were binned to 0.08 Å.

3 SPECTRAL ANALYSIS

3.1 Stellar atmosphere models

Our well-established technique for the analysis of high-resolution spectra is discussed in detail in Cruddace et al. (2002). In this paper we extend the range of spectral models used, as listed in Table 1. Models 1–3 were computed using the stellar atmosphere code TLUSTY and its associated spectral synthesis codeSYNSPEC (Hubeny & Lanz 1995; Lanz et al. 1996), which consider homogeneous mixtures of He and heavy elements besides more complex stratified distributions of materials (see Table 1, models 1–3). Model 4 is a small grid of calculations using a variant of the PRO2 code (Werner & Dreizler 1999; Werner et al. 2003), where the balancing effects of radiative levitation and downward gravitational diffusion are taken into account in a self-consistent way (Dreizler & Wolff 1999; Schuh et al. 2002). These models should give a much better physical description of the atmospheric structure than the empirical 'slab' type model 3. $T_{\rm eff}$ ranged from 53 000 to 56 000 K and $\log g$ from 7.4 to 7.6. Because the atmospheric structure and depth-dependent abundances are a function of both $T_{\rm eff}$ and $\log g$, these parameters were allowed to vary freely within the limits during the analysis. As before, interstellar opacity was taken into account with our modified version of the Rumph, Bowyer & Vennes (1994) model.

For all the TLUSTY models, we fixed the stellar temperature and surface gravity ($T_{\rm eff}$ = 54 000 K, $\log g$ = 7.5) at the grid points closest to the values determined from the Balmer and Lyman lines of G191-B2B (Barstow et al. 1998). Apart from the helium and Fe abundances, which were allowed to vary freely between the grid limits of 10^{-4} and 10^{-6} and 3.0×10^{-5} and 3×10^{-6}, respectively, the homogeneous abundances of the heavy elements were fixed at values determined from far-UV observation (C/H = 4.0×10^{-7}, N/H = 1.6×10^{-7}, O/H = 9.6×10^{-7}, Si/H = 3.0×10^{-7}, Ni/H = 5.0×10^{-7}), to allow direct comparison with the results from our earlier analysis of the *J-PEX* spectrum. However, Barstow et al. (2003) have subsequently reanalysed the STIS spectrum of G191-B2B and revised these values. Therefore, we have included in this analysis another uniform model (model 5), with variable He and Fe abundances and the new STIS abundances for the other heavy elements.

Table 1. Summary of theoretical model atmosphere calculations used for the analyses in this paper, giving details of temperature, gravity and abundances for each grid.

No	Description	$T_{\rm eff}$ (K)	$\log g$	Helium treatment	Heavy element treatment
1	Fully homogeneous	54 000	7.5	He/H 10^{-6}–10^{-4}	Fe/H from 3×10^{-6} to 3×10^{-5}, others with fixed uniform abundances (see text)
2	Stratified H+He	54 000	7.5	H mass 10^{-14}–10^{-13}	As for model 1
3	Barstow et al. (1999) stratified Fe	54 000	7.5	H mass 10^{-14}–10^{-13}	Fe from fe4 to fe6 models, others with fixed uniform abundances (see text)
4	PRO2 self-consistent rad. lev. & diffusion	53 000–56 000	7.4–7.6	Determined by self-consistent calculation of radiative levitation and diffusion effects for given $T_{\rm eff}$ and $\log g$	
5	Fully homogeneous	54 000	7.5	He/H 10^{-6}–10^{-4}	Fe/H from 3×10^{-6} to 3×10^{-5}, others fixed at STIS values (see text)

3.2 Analysis procedures

For all this work, the interstellar H I and He I column densities were fixed at values obtained from analysis of the broader-band, lower-resolution *EUVE* spectrum by Barstow et al. (1999), adopting values from the closest similar model used in the *EUVE* work. Columns of H I = 2.15 × 10^{18} cm^{-2} and He I = 2.18 × 10^{17} cm^{-2}, determined using a homogeneous atmosphere model were adopted for models 1 and 5, while columns of H I = 2.05 × 10^{18} cm^{-2} and He I = 2.00 × 10^{17} cm^{-2}, corresponding to the fe6 stratified model of Barstow et al. (1999), were used with all the stratified calculations (models 2, 3 and 4). The He II column density was always allowed to vary freely and independently of the other interstellar components.

Our initial analysis of the *J-PEX* spectrum of G191-B2B, reported by Cruddace et al. (2002), made the assumption that the interstellar He II present existed as a single component. However, far-UV spectroscopy has revealed that there are two components to the interstellar medium (ISM). One of these is associated with the local interstellar cloud (LIC), while the other is designated component I (see Sahu et al. 1999). Component I is very similar in velocity to highly ionized, possibly circumstellar, material revealed through the detection of a C IV doublet near 1550 Å (Vennes & Lanz 2001; Bannister et al. 2003), which is blueshifted with respect to the photospheric velocity. While the velocity separation of the LIC and stellar photosphere is small (∼4.6 km s^{-1}) and well below the resolving power of the *J-PEX* spectrograph, the difference between component I and the stellar photosphere is much larger at 16.6 km s^{-1}. We would not expect to resolve these components because this is still below the instrument resolution (equivalent to ∼75 km s^{-1} FWHM), but the quality of the agreement between model and observation could be affected, through an apparent broadening of the He lines, if not taken into account. Therefore, we treat the He II opacity as being provided by two discrete components, each having a different velocity and column density. Both parameters of each component were allowed to vary independently during the spectral analysis.

An inspection of the original analysis of the *J-PEX* spectrum shows that the match between the wavelengths of detected features with their predicted location is not always satisfactory. For example, this is apparent near the He II Lyman series limit near 228 Å, where an apparent emission feature appears about two-wavelength bins (0.1 Å) shortward of its location in the model. This peak is a residual of the continuum in a region containing a number of overlapping He II interstellar absorption features. Similar discrepancies are found elsewhere, indicating that there are small residual errors in the wavelength calibration. Because we do not have any additional calibration information to deal with this, we have assumed that the predicted wavelengths of the peak near 228 Å and certain well-known and reliable absorption features are correct, and have adjusted the wavelength calibration accordingly. In doing this, any absolute velocity information is compromised, but relative velocities (say between photospheric and ISM components) are preserved. It is important to note that most published EUV wavelengths are calculated rather than measured and are not necessarily accurate. This is particularly true of complex atoms having many millions of EUV lines, such as Fe or Ni. However, for low *Z* elements this is much less of a problem. We list here the lines that we have used, highlighting the strong positive detections in bold type and the weaker, less certain, features in normal type: He II (λλ 228.06, 228.54, 230.14), C IV (λ 238.25), N IV (λλ 238.07), O IV (λλ 231.7, 231.25, 233.47, 233.56, 238.57) and O V (λλ 227.51, 231.82).

As reported in our original paper, some strong absorption features in the spectrum of G191-B2B are not predicted by our white dwarf atmosphere models, despite the inclusion of the more abundant elements and a very comprehensive library of spectral transitions. Because they can potentially alter the fit between model and data by forcing the procedure to average out the flux differences across the line, which might yield some erroneous results, we have excluded those regions of the spectrum where the strongest such features occur from the analysis. Specifically, these are at 229.15 and 232.75 Å and appear as gaps in Figs 1(a) and (b). In addition, we have not used the very shortest wavelength part of the spectrum below 226 Å (or a section near 227.5 Å), where there are many bins containing zero counts, because these cannot be handled by the fitting algorithm. In other regions of the spectrum where similar discrepancies can be seen, we have not excluded the data points because a feature is predicted at the specific wavelength, but not as strong or weak as actually observed.

3.3 Spectral analysis results

As the groups of models with homogeneous or stratified heavy element compositions give rather similar results, Figs 1 and 2 show the best match between the data and two representative models: model 5 (Figs 1a and 2a) and model 4 (Figs 1b and 2b). Table 2 lists the values of all the parameters for these.

In general, all the models give a reasonably good agreement with the data, but formally, the fits to stratified models 3 and 4 are not acceptable. All the best-fitting models include opacity from both photospheric and interstellar helium, the levels of photospheric opacity being consistent with our inability on this flight to achieve positive detections in the 237.331- and 243.026-Å He II lines. Furthermore, no significant change in the quality of the fit is noted if the photospheric component is forced to zero and all the He II opacity assumed to be interstellar and/or circumstellar. Compared to our initial analysis, the match between the locations of absorption features in the observed spectrum and those of the models is much improved. Particularly good agreement is obtained in the ∼228 to 230 Å wavelength range. Apart from the He II Lyman series, no strong absorption lines are predicted by the models in this range. We can clearly identify λ228.54 (left-hand arrow in Fig. 1a), and blends of He lines down to the series limit (marked by the bracket in Fig. 1a). The apparent emission feature at 227.9 Å is an artefact of the effect of He II line series opacity on the stellar emission, which was predicted by our modelling before the *J-PEX* flight. The absorption line at 229.0 Å coincides with predicted He II and O III features and is probably a blend of both (right-hand arrow in Fig. 1a).

4 DISCUSSION

4.1 Homogeneous versus stratified heavy element distributions

Because it is accepted that the presence of significant quantities of heavy elements in the atmospheres of hot DA white dwarfs such as G191-B2B is a result of radiative levitation, it is a surprise that the best agreement with the *J-PEX* spectrum is obtained with models having a homogeneous distribution of material. In particular, this result contradicts the analyses of the *EUVE* spectrum of G191-B2B, which require a stratified atmospheric structure to reconcile the overall spectral shape across the full ∼100–600 Å wavelength range, in particular at wavelengths below 190 Å (Barstow et al. 1999; Dreizler & Wolff 1999). This is a problem of detail versus global coverage. The *EUVE* spectrum covers a broad wavelength range (∼500 Å)

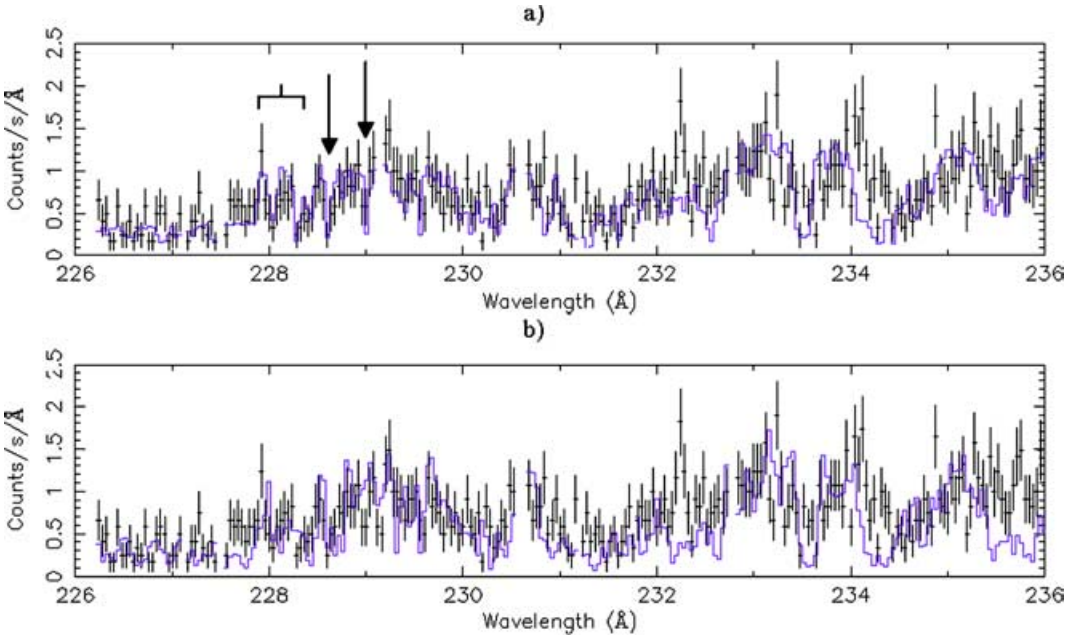

Figure 1. Comparison of the best-fitting spectral models for each atmosphere type (histograms) with the 226–236 Å region of the *J-PEX* spectrum of G191-B2B (error bars). (a) Homogeneous mixture of all elements – model 5. (b) Self-consistent radiative levitation/diffusion PRO2 model – model 4. In (a) the bracket identifies the converging He II Lyman series lines and the series limit, the left arrow marks He II 228.54 Å and the right arrow a blended feature of O III and He II at 229.0 Å.

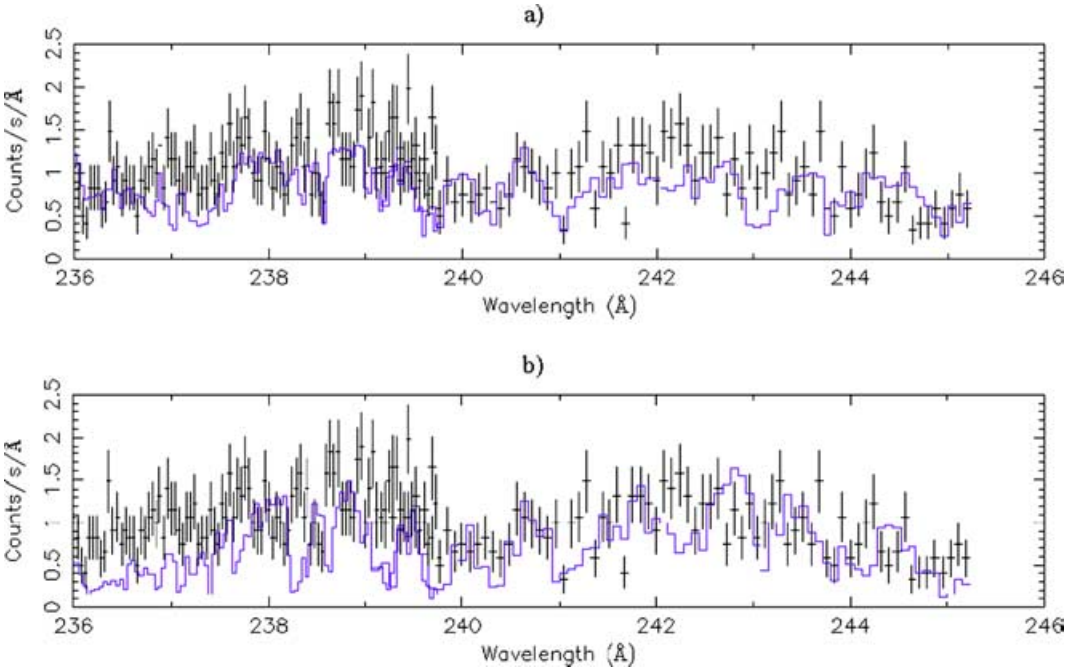

Figure 2. Comparison of the best-fitting spectral models for each atmosphere type (histograms) with the 236–246 Å region of the *J-PEX* spectrum of G191-B2B (error bars). From the top, (a) homogeneous mixture of all elements – model 5. (b) Self-consistent radiative levitation/diffusion PRO2 model – model 4.

and with much better signal-to-noise than the *J-PEX* spectrum, but has limited (∼0.5 Å) spectral resolution. In contrast, *J-PEX* has a much narrower band (∼25 Å) but a factor of 10 better resolving power. Inspection of Figs 1 and 2 reveals that, over the *J-PEX* waveband, the stratified models have too much opacity, particularly at the longer wavelengths above 235 Å. In fact, this is also the case in the *EUVE* analyses. The individual features predicted at the resolution of *EUVE* are generally stronger than in the data. Hence, even before the *J-PEX* flight the problem of reconciling the predicted detailed line opacity with that observed already existed, but was given secondary consideration compared to the reproduction of the overall spectral shape by the models.

As we would expect to obtain consistency between the two instruments, this is probably an indication of current limitations in the

Table 2. Summary of the results of the various analyses of the *J-PEX* spectrum of G191-B2B as discussed in the text, for two representative model structures/compositions. The parameter z is the measured redshift for the various opacity components considered.

	Model number and description			
	Model 4. Self-consistent levitation/diffusion	Model 5. Fully homogeneous with STIS heavy element abundances		
			-1σ	$+1\sigma$
$T_{\rm eff}$ (K)	53 000	54 000		
log g	7.6	7.5		
He II ISM A (LIC?) (cm^{-2})	3.20×10^{17}	2.58×10^{17}	1.47×10^{17}	1.95×10^{17}
He II ISM B (LB?) (cm^{-2})	2.70×10^{17}	4.55×10^{17}	1.85×10^{17}	1.55×10^{17}
He/H (number) or H mass ($M_\odot$)	n/a	3.00×10^{-5}	7.60×10^{-6}	1.17×10^{-5}
Fe/H (number)	n/a	8.26×10^{-7}	2.51×10^{-7}	2.94×10^{-7}
$z_{\rm LIC}$	-4.77×10^{-5}	1.51×10^{-5}	1.30×10^{-6}	1.30×10^{-6}
$z_{\rm ISM}$	-1.00×10^{-4}	-6.23×10^{-5}	1.10×10^{-6}	1.10×10^{-6}
$v_{\rm ISM-LIC}$ (km s^{-1})	-15.69	-23.22	0.51	0.51

models. It is likely that there are deficiencies in the atomic data used, because the wavelengths and oscillator strengths are largely calculated rather than measured. Any inaccuracies in these computations would be reflected in incorrect opacities and implied abundances. This is particularly true for Fe and Ni lines, the dominant sources of photospheric opacity.

Furthermore, the inability of the models to account for some of the stronger lines detected is an indication that the input data are incomplete. For the stratified models, their main observational deficiency is that the photospheric lines and complexes are typically predicted to be stronger than observed across the whole *J-PEX* waveband. Of particular note are broad regions at 234.5–236 Å (see Fig. 1b) and 236–237 Å, besides narrow complexes at ∼238.3 and 239.3 Å (see Fig. 2b), all associated with groups of Fe and Ni lines. Revised atomic data might rectify this. Alternatively, the radiative levitation calculations may predict abundance profiles that are not sufficiently accurate to reproduce the observed opacity, at the depths where the observed lines are formed. These abundances are 'fixed' by the stellar parameters and cannot be fine-tuned with the freedom available in the homogeneous models, which might explain why these are a better match across the narrower spectral range. These results indicate that the actual element abundances are lower, at the line formation depth, than the radiative levitation calculations predict, but they do not demonstrate that the heavy elements are not stratified.

Other physical effects may eventually need to be included to provide more realistic models. Mass loss could contribute to a relative depletion of the heavy element material and modify the stratification, bringing the *EUVE* and *J-PEX* analyses into closer agreement.

4.2 Interstellar and/or circumstellar He II

All EUV studies of G191-B2B require an interstellar component (or components) of He II opacity to explain the observed spectra, in combination with either homogeneous or stratified models. At the resolution of *EUVE* and in the presence of absorption from many other species, this material could not be directly detected. However, the *J-PEX* data clearly reveal the interstellar He II Lyman series lines, and further they imply that there is a contribution from photospheric He. In our new analysis we have divided the ionized interstellar He into two contributions, identified with the LIC and ISM component I. The fitting procedure naturally separates these two components in velocity space, the velocity difference of ~ -23 km s^{-1} (Table 1) being similar to the ~ -14 km s^{-1} reported by Sahu et al. (1999). However, both this value and the formal error in the velocity (∼0.5 km s^{-1}) are small, compared to the velocity resolution of 75 km s^{-1}. However, using the information available through the existing high-resolution STIS spectra, we can assume that there are two interstellar/circumstellar absorption components along the line of sight, and we have obtained measurements of the respective column densities and the formal uncertainties. All of the error ranges listed in Table 1 exclude a zero column density for either component, but these are only 1σ limits, corresponding to a confidence limit of 68 per cent. If we apply a more stringent 3σ criterion, then a zero column density does lie within the error bounds. Our resolving power (∼4000) is considerably lower than that of STIS ($R = 40\,000$–$100\,000$), which prevents determination of the velocity differences between the components, which are below the discrimination possible with *J-PEX*. Therefore, the evidence in the *J-PEX* spectrum for the presence of two interstellar/circumstellar components is not conclusive.

Nevertheless, using the far-UV evidence that two ISM components are present we consider the implication that the EUV opacity we observe is divided between these two components. A problem in earlier studies of G191-B2B has been the high He II ionization fraction obtained from a single absorbing component, in comparison with other lines of sight in and around the LIC and the Local Bubble. Combining the two He II components treated here into a single one yields a similar result to earlier analyses, namely an ionization fraction [$N_{\rm He\,II}/(N_{\rm He\,II}+N_{\rm He\,I})$] of 0.77 for the best homogeneous model (model 5). Similar fractions (within ±0.04) are obtained for the other models within the $\sim \pm 10$ per cent uncertainty of the estimate (based on the He II column uncertainties alone, the uncertainty in the He I measurement has not been quantified).

If we consider the two components individually, we have to make some assumptions about how He I is distributed between the two regions, the LIC and component I, because the wavelength coverage of *J-PEX* does not include the 206-Å He I line. Bannister et al. (2003) have pointed out the association of the latter with highly ionized material seen in the STIS spectrum. Hence, the most extreme case we can consider, with all the neutral helium residing in the LIC and the medium outside the LIC associated with component I being completely ionized, would seem to be a good approximation to the existing conditions. The best fits for the models yield a large spread in the ionization fraction of the LIC, ranging from 0.43 (model 2) to 0.68 (model 3). Model 5, the homogeneous model with revised heavy element abundances yields a value of 0.54. In

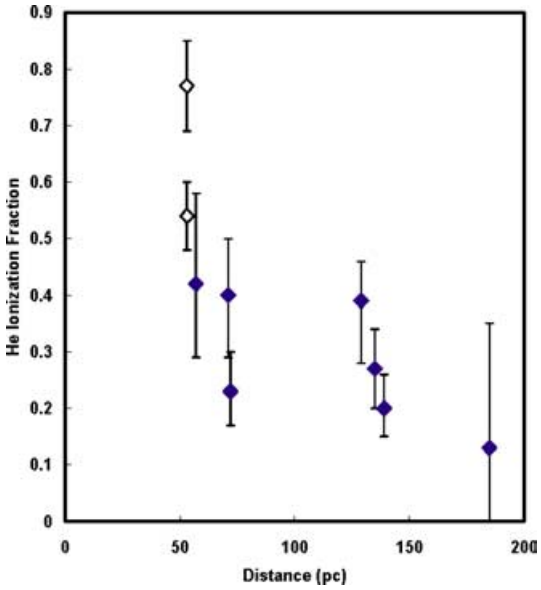

Figure 3. Comparison of our results for G191-B2B (from model 5, open diamonds) with those of Barstow et al. (1997, filled diamonds), showing the calculated ionization fraction as a function of stellar distance. For G191-B2B, the upper symbol is the ionization fraction estimate for the total He II column, while the lower of the two is that calculated for the LIC, assuming all the neutral helium resides therein, as discussed in the text.

Fig. 3, which shows the calculated ionization fraction as a function of stellar distance (estimated photometrically), we compare our results for G191-B2B (open diamonds) with those of Barstow et al. (1997, filled diamonds), who reported *EUVE* observations including a number of stars with pure H atmospheres. For G191-B2B, the upper symbol is the ionization fraction estimate for the total He II column, while the lower of the two is that calculated for the LIC, assuming all the neutral helium resides there, as discussed above. This lower value is consistent with the Barstow et al. (1997) results, within the overall uncertainties, and supports the argument that there are two He II components in the line of sight to G191-B2B.

5 CONCLUSION

We have presented a detailed analysis of the high-resolution EUV spectrum of G191-B2B, obtained with the sounding rocket-borne *J-PEX* spectrometer. This new work confirms the basic results of the initial analysis, published by Cruddace et al. (2002), but incorporates an improved treatment of the wavelength calibration, considers a wider range of possible atmosphere models and examines multiple interstellar components. We find that homogeneous atmospheres fit the *J-PEX* high-resolution EUV spectra better than stratified models. This contradicts earlier analyses of EUVE spectra, and the discrepancy is attributed to one or both of two possible reasons: deficiencies in atomic data for the some 10^7 absorption lines used in the models, incompleteness of the models, for example the effects of mass loss from the atmosphere.

Dividing the interstellar He II absorption into two components, one in the LIC, yields a better fit to the *J-PEX* EUV spectrum and solves the problem of the high ionization fraction (>0.7) deduced from earlier single component studies. The *J-PEX* result is not conclusive but is consistent with studies made with STIS.

ACKNOWLEDGMENTS

MAB and NPB were supported by the UK Particle Physics and Astronomy Research Council (PPARC). The Naval Research Laboratory (NRL) was supported in this work by the National Aeronautics and Space Administration (NASA) under grant NDPR S-47440F and by the Office of Naval Research under NRL work unit 3641 (Application of Multilayer Coated Optics to Remote Sensing). SS was supported by DFG grants DR 281/13-1 and DR 281/13-2 to the University of Tübingen. SS also acknowledges PPARC and the Schuler Stiftung for travel support in association with this work.

REFERENCES

Bannister N. P., Barstow M. A., Holberg J. B., Bruhweiler F. C., 2003, MNRAS, 341, 477
Barstow M. A., Dobbie P. D., Holberg J. B., Hubeny I., Lanz T., 1997, MNRAS, 286, 58
Barstow M. A., Hubeny I., Holberg J. B., 1998, MNRAS, 299, 520
Barstow M. A., Hubeny I., Holberg J. B., 1999, MNRAS, 307, 884
Barstow M. A., Good S. A., Holberg J. B., Hubeny I., Bannister N. P., Bruhweiler F. C., Burleigh M. R., Napiwotzki R., 2003, MNRAS, 341, 870
Cruddace R. G. et al., 2002, ApJ, 565, L47
Dreizler S., Wolff B., 1999, A&A, 352, 632
Holberg J. B., Hubeny I., Barstow M. A., Lanz T., Sion E. M., Tweedy R. W., 1994, ApJ, 425, L205
Hubeny I., Lanz T., 1995, ApJ, 439, 875
Lanz T., Barstow M. A., Hubeny I., Holberg J. B., 1996, ApJ, 473, 1089
Rumph T., Bowyer S., Vennes S., 1994, AJ, 107, 2108
Sahu M. S. et al., 1999, ApJ, 523, L159
Schuh S., Dreizler S., Wolff B., 2002, A&A, 382, 164
Sion E. M., Bohlin R. C., Tweedy R. W., Vauclair G., 1992, ApJ, 391, L29
Vennes S., Lanz T., 2001, ApJ, 553, 399
Vennes S., Chayer P., Thorstensen J. R., Bowyer C. S., Shipman H. L., 1992, ApJ, 392, L27
Werner K., Dreizler S., 1999, J. Comput. Appl. Math., 109, 65
Werner K., Deetjen J. L., Dreizler S., Nagel T., Rauch T., Schuh S. L., 2003, in Hubeny I., Mihalas D., Werner K., eds, ASP Conf. Ser. Vol. 288, Stellar Atmosphere Modelling. Astron. Soc. Pac., San Francisco, p. 31

This paper has been typeset from a TEX/LATEX file prepared by the author.